Optica Applicata, Vol. XVII, No. 2, 1987

Effect of third-order aberrations on the point spread function of a polarizing microscope with crossed polarizers

JAGPAL SINGH*, K. SINGH

Physics Department, Indian Institute of Technology, Delhi, New Delhi–110016, India.

The effect of third-order aberrations (spherical, coma and astigmatism) on the intensity distribution in the images of a point object has been examined for the polarizing microscope with crossed polarizers. Detailed results, showing the deterioration of the image in the presence of aberrations have been given for the decrease of intensity in the main lobe and broadening of the image. The extent of improvement in the presence of defocusing for the system with spherical aberration has been illustrated. In the presence of coma, the shift in the position of the peak of the main lobe increases with increasing amount of coma.

1. Introduction

A polarizing microscope is used for studying the birefringence of objects and for rendering the objects visible according to their optical anisotropy. Based on Fourier-transform techniques, numerous investigations have been carried out concerning the diffraction images of various extended objects under different conditions of illumination [1]–[10]. The basic theory of image formation in a polarizing microscope has been discussed by KUBOTA and his co-workers [1], [2] who showed that the diffraction image of a point formed by an aberration-free system is different from the conventional Airy disc. Therefore, the performance of the system cannot be analysed by applying Rayleigh or Strehl criterion. Recently, BARAKAT [10] has extensively studied the imaging of extended objects and obtained for cumulative point spread, line spread and the edge spread functions closed form solutions in terms of the Lommer–Weber and Struve functions. GUPTA et al. [9] calculated the images of extended objects by suitably integrating the point spread function.

In all the above references, the system is considered to be aberration-free. However, the lenses used in the practical system are never diffraction-limited. Therefore, the studies of optical system under realistic condition of aberrations are of practical importance. The influence of aberrations and defocussing on the performance of various optical systems has been a subejct of long standing study

* Present address: Harvin Optical and Glass Industries, C–34, Sanat Nagar Industrial Estate, Hyderabad–500018.

and a variety of methods have been used to tackle the problem of calculating the intensity distribution in the images. An excellent summary of earlier works on the subject is given by BORN and WOLF [11]. The detailed study of various image assessment parameters (i.e., point image, line image, edge image, flux through hole and slit and frequency response) for the third-order aberrations has been published by KAPANY and BURKE [12]. In the presence of off-axis aberrations, the line and edge spread functions have been evaluated by BARAKAT and HOUSTON [13]. YOSHIDA and ASAKURA [14] presented the results for the diffraction pattern of off-axis Gaussian beam formed by an optical system with astigmatism. GUPTA et al. [15] and GUPTA and SINGH [16] investigated respectively the effect of coma and astigmatism on the images of extended objects like disk and annulus. A number of other relevant references can be found in [15], [16].

The effect of aberrations on the imaging properties of optical systems, like catadioptric and scanning optical microscope, have also been studied respectively by POVELL [17] and SHEPPARD and WILSON [18]. HOFMANN and PABST [19] demonstrated the method for plotting the wave-front and point spread function in three-dimensions. As it is well known that the sources are never completely monochromatic, the effect of off-axis aberration on the point spread function in polychromatic light has been investigated by YZUEL and BESCOS [20]. The results for the combined effect of apodization and aberration on the performance of optical system have been given by BISWAS and BOIVIN [21], [22], HAZRA [23], YZUEL and CALVO [24] and MAGIERA et al. [25], [26].

In recent years, the Zernike polynomial description has turned out to be very important from the point of view of aberration balancing and an excellent summary of earlier works on this subject is given by BORN and WOLF [11]. The advantages of Zernike polynomials and the principal areas of their applications have been pointed out by TANGO [27], BARAKAT [28] extended and generalized the theory for constant amplitude circular aperture to the case of an annular aperture. BUDGOR [29] derived an exact relationship for scalar diffraction theory of aberration.

In all the above mentioned methods, the accuracy of computation plays a very important part. A series of research papers on different computational schemes has been published recently [30]–[34] and a detailed analysis has been presented by BARAKAT [31]. YZUEL and ARLEGUE [32] have also paid special attention to the accuracy in the numerical evaluation.

In the present paper, we have obtained numerical results for the point spread function of the polarizing microscope with crossed polarizers in the presence of third-order aberrations.

2. Theory

The point spread function of an optical system can be evaluated by taking the modulus square of the Fourier transform of the pupil function. The pupil function of the system is itself a function of the design data of the lens system. Therefore, the point spread function of the system, when the aberrations are present, is of considerable importance.

The pupil function which specifies the complex amplitude over the exit pupil of the optical system is written as

$$f(x, y) = A(x, y) \exp\{i\bar{k}W(x, y)\}. \tag{1}$$

Here $A(x, y)$ describes the variation in amplitude over the image forming wavefront and is zero outside the domain of the pupil, $W(x, y)$ is the wavefront aberration at the point x, y and $\bar{k} = 2\pi/\lambda$.

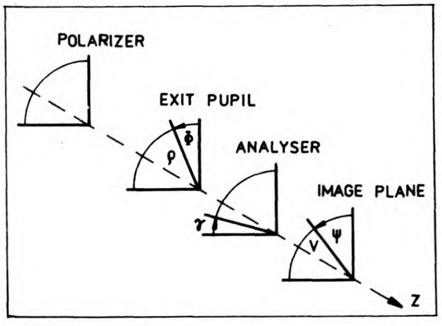

Fig. 1. Schematic optical system

If we consider the geometry of the polarizing microscope (Fig. 1) when polarizers are crossed, the amplitude variation of the pupil can be written as [1]

$$A(\varrho, \Phi) = \frac{1}{2}[k_{\parallel}(\varrho) - k_{\perp}(\varrho)] \sin 2\Phi \tag{2}$$

where (ϱ, Φ) are the polar coordinates in the exit pupil, $k_{\parallel}(\varrho)$ and $k_{\perp}(\varrho)$ are the amplitude loss factors of the optical system for the components of light polarized parallel and perpendicular to the plane of incidence and are the function of ϱ, only. $k_{\parallel}(\varrho) \pm k_{\perp}(\varrho)$ can be expressed into a series of circular polynomials [1] and can be written as

$$k_{\parallel}(\varrho) - k_{\perp}(\varrho) = \alpha\varrho^2 + \beta\varrho^4 + \gamma\varrho^6 + \ldots . \tag{3}$$

It has been proved from experimental data [1] that for a small numerical aperture system $\alpha \gg \beta$. Therefore, we can write

$$A(\varrho, \Phi) = \varrho^2 \sin 2\Phi. \tag{4}$$

The aberration function $W(\varrho, \Phi)$ for the defocusing and third-order aberration is

$$W(\varrho, \Phi) = W_{20}\varrho^2 + W_{40}\varrho^4 + W_{31}\varrho^3 \cos\Phi + W_{22}\varrho^2 \cos^2\Phi. \tag{5}$$

W_{20}, W_{40}, W_{31} and W_{22} are the coefficients of defocusing, third-order spherical aberration, coma and astigmatism, respectively.

Therefore, the pupil function in the presence of third-order aberration is written as

$$f(\varrho, \Phi) = \varrho^2 \sin 2\Phi \exp\{i\bar{k}(W_{20}\varrho^2 + W_{40}\varrho^4 + W_{31}\varrho^3 \cos\Phi + W_{22}\varrho^2 \cos^2\Phi)\}. \tag{6}$$

The intensity distribution in the point spread function can be written as

$$I(V, \Psi) = \left| \frac{1}{c} \int_0^1 \int_0^{2\pi} f(\varrho, \Phi) \exp\{iV\varrho\cos(\Psi - \Phi)\} \varrho d\varrho d\Phi \right|^2 . \tag{7}$$

The point spread function can also be evaluated by taking the inverse Fourier-transform of the optical transfer function, which is the auto-correlation of the pupil function.

For rotationally symmetric third-order aberrations, i.e., W_{20} and W_{40}, the above equation can be written as

$$I(V, \Psi) = \left|2\pi i^2 \sin 2\Psi \int_0^1 J_2(V\varrho)\varrho^2 \exp\{i\bar{k}(W_{20}\varrho^2 + W_{40}\varrho^4)\} \varrho d\varrho\right|^2 . \tag{8}$$

For the case of defocusing (W_{20}) it is possible to evaluate this integral in terms of Lommel functions [35], namely

$$I(V, \Psi) = \left|2\pi i^2 \sin 2\Psi \int_0^1 J_2(V\varrho)\varrho^2 \exp(i\bar{k}W_{20}\varrho^2) \varrho d\varrho\right|^2 . \tag{9}$$

The generalized Lommel–Weber function is defined as

$$W_m^\nu(\gamma, \mu) = \int_0^1 (1-\xi^2)^\nu J_m(\mu\xi) \exp\left\{i\frac{\gamma}{2}(1-\xi^2)\right\} \xi^{m+1} d\xi . \tag{10}$$

For $\nu = 0$, $m = 2$ the Eq. (10) can be written as

$$W_2^0(\gamma, \mu) = \int_0^1 J_2(\mu\xi) \exp\left\{i\frac{\gamma}{2}(1-\xi^2)\right\} \xi^3 d\xi . \tag{11}$$

If we multiply and divide the Eq. (9) by $\exp(i\bar{k}W_{20})$, it will be changed to

$$I(V, \Psi) = |2\pi i^2 \sin 2\Psi \exp\{i\bar{k}W_{20} \int_0^1 J_2(V\varrho)\} \exp\{-i\bar{k}W_{20}(1-\varrho^2)\} \varrho^3 d\varrho|^2 . \tag{12}$$

On comparing the integrals of Eq. (11) with (12), we can write

$$I(V, \Psi) = |2\pi i^2 \sin 2\Psi \exp\{i\bar{k}W_{20}\} W_2^0(\zeta, V)|^2 \tag{13}$$

where $\zeta = -2\bar{k}W_{20}$. The relation between the generalized Lommel–Weber and Lommel function of two variables is the following:

$$W_m^0(\gamma, \mu) = \frac{\mu^m}{\gamma^{m+1}} [U_{m+1}(\gamma, \mu) + iU_{m+2}(\gamma, \mu)] \tag{14}$$

where $U_m(\gamma, \mu)$ is defined as

$$U_m(\gamma, \mu) = \sum_{s=0}^{\infty} (-1)^s \left(\frac{\gamma}{\mu}\right)^{m+2s} J_{m+2s}(\mu) . \tag{15}$$

Therefore

$$W_2^0(\zeta, V) = \frac{V^2}{\zeta^3}[U_3(\zeta, V) + iU_4(\zeta, V)]. \tag{16}$$

The expression for the intensity distribution can now be written as

$$I(V, \Psi) = 4\pi^2 \sin 2\Psi \frac{V^4}{\zeta^6}[U_3^2(\zeta, V) + U_4^2(\zeta, V)] \tag{17}$$

where U_3 and U_4 are the Lommel functions of orders 3 and 4.

3. Results and discussion

The point spread function given by Eq. (7) has been evaluated numerically on an ICL–2960 computer by using Gauss quadrature with 24-points. The intensity distributions in the images of a point object for different values of the aberration coefficients and $\Psi = \pi/4$ for W_{20} and W_{40} and $\Psi = \pi/8$ and $\pi/4$ for W_{31} and W_{22} have been shown in Figs. 2–6. For $\Psi = 0.0$, the numerical values are so small that the curves have not been plotted. For an aberration-free case the maximum intensity is normalized to unity and shown with dotted curves.

3.1. Defocusing and spherical aberration

Figure 2 shows the effect of defocusing on the point spread function of the polarizing microscope for $\Psi = \pi/4$ and $W_{20} = 0.0$, 0.25λ, 0.50λ, 0.75λ and 1.0λ. The position of the primary maximum is not affected by the aberration parameters.

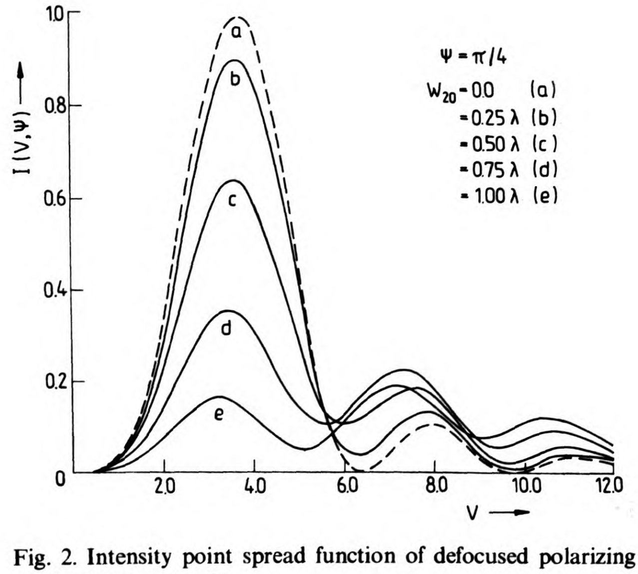

Fig. 2. Intensity point spread function of defocused polarizing microscope: $\Psi = \pi/4$; $W_{20} = 0.0$, 0.25λ, 0.50λ, 0.75λ and 1.0λ

The increase in W_{20} causes reduction in the main lobe of the diffraction pattern, while the higher-order lobes become brighter. The basic structure of the point spread function cannot be predicted for higher values of W_{20}, say $W_{20} = 1.0\lambda$. Results obtained from Eq. (7) by computation, checked by evaluating Eq. (17) at few values of V and W_{20}, were found to be in good agreement.

Figure 3 shows the point spread function in the presence of primary spherical

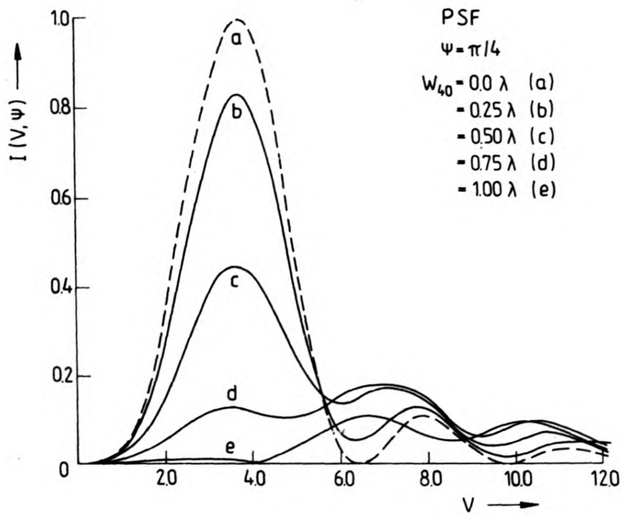

Fig. 3. Intensity point spread of polarizing microscope in the presence of third-order spherical aberration: $\Psi = \pi/4$; $W_{40} = 0.0$, 0.25λ, 0.50λ, 0.75λ and 1.0λ

aberration. The behaviour of the curves is similar in nature to those of Fig. 2. However, the degradation in the point spread function is more rapid than in the case of W_{20} for the same value of the aberration coefficient.

Figures **4a–c** show the combined effect of the defocusing and third-order spherical aberration. There is a marked improvement (Fig. **4a**) in the image sharpness for $W_{20} = -0.25\lambda$ and $W_{40} = 0.25\lambda$, resulting in the point spread curves substantially similar to the one for aberration-free case. Similarly, in Fig. **4b**, a considerable improvement results for $W_{20} = -0.50\lambda$ and $W_{40} = 0.50\lambda$. For larger aberrations (Fig. **4c**), slight improvement has also been noticed. From the trend of the curves, we can see that the best focal plane for this case is $W_{40} = -W_{20}$.

3.2. Coma and astigmatism

The results obtained by us in paraxial receiving plane along $\Psi = \pi/8$ and $\pi/4$ for $W_{31} = 0.0$, 0.25λ, 0.50λ, 0.75λ and 1.0λ are shown in Figs. **5a**, **b**. It is observed that the position of the maximum intensity in aberrated cases is displaced from the position in the case of aberration-free system. Shift becomes maximum along $\Psi = \pi/4$. The shift increases almost linearly with the increasing magnitude of the aberration. In the presence of aberration the intensity distribution is highly

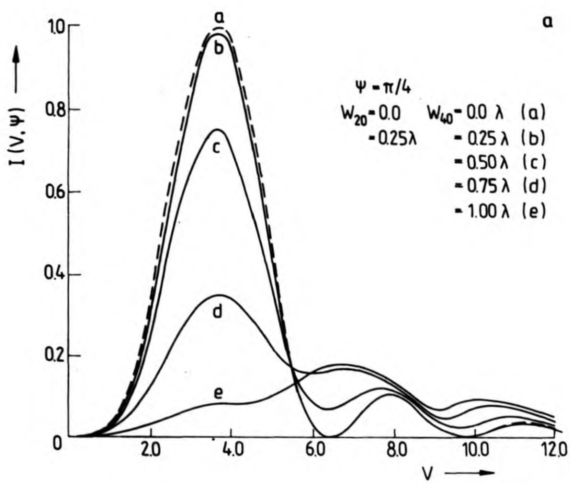

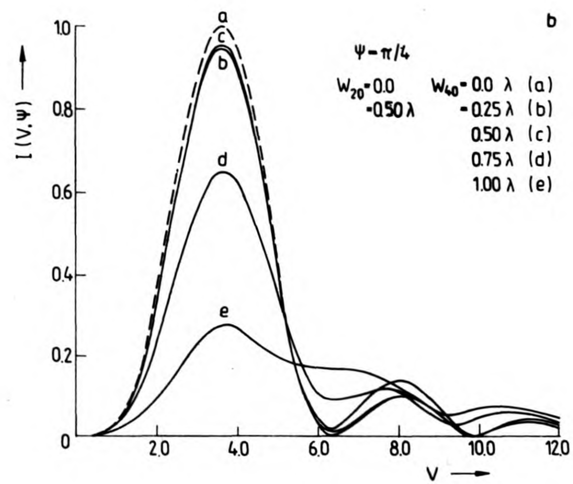

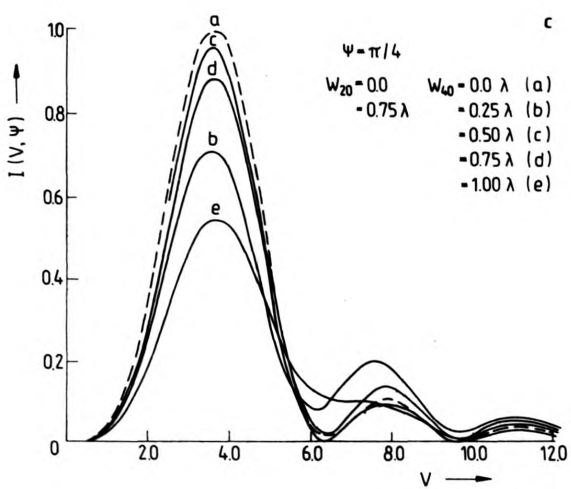

Fig. 4. Intensity point spread function of polarizing microscope for $\Psi = \pi/4$: **a** – $W_{20} = -0.25\lambda$, $W_{40} = 0.25\lambda$, 0.50λ, 0.75λ and 1.0λ, **b** – $W_{20} = -0.50\lambda$, W_{40} – the same as in **a**, **c** – $W_{20} = 0.75\lambda$, W_{40} – the same as in **a**

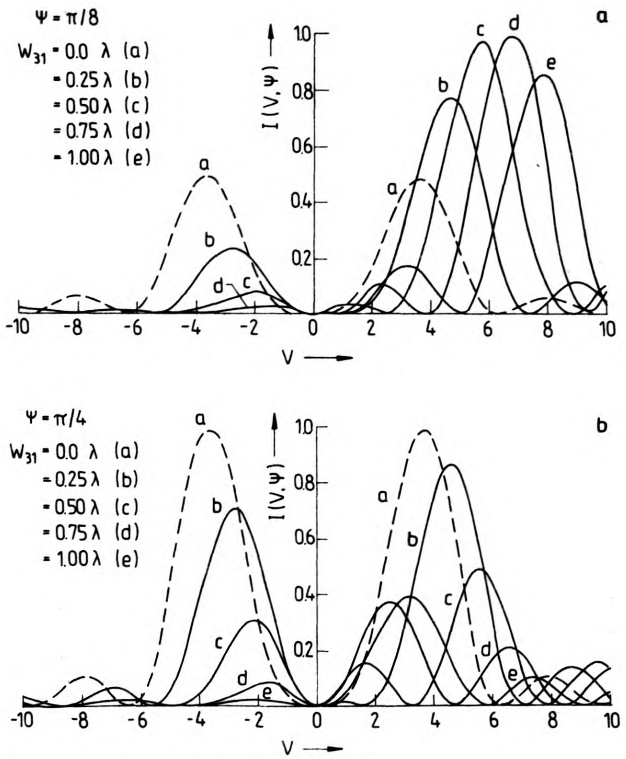

Fig. 5. Intensity point spread function of polarizing microscope in the presence of primary coma: **a** – $\Psi = \pi/8$, $W_{31} = 0.0$, $0{,}25\lambda$, 0.50λ, 0.75λ and 1.0λ, **b** – $\Psi = \pi/4$, W_{31} – the same as in **a**

asymmetric with respect to the origin. There is also a decrease of intensity in the main lobe. The intensity at $V = 0.0$ is zero.

Figures 6**a**, **b** show the intensity distribution in the point spread function for

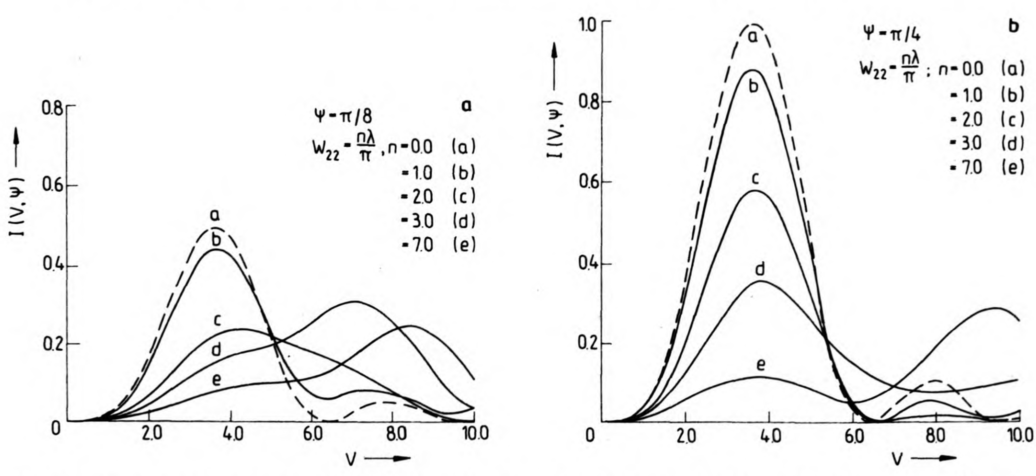

Fig. 6. Intensity point spread function in the presence of primary astigmatism: **a** – $\Psi = \pi/8$, $W_{22} = n\lambda/\pi$, $n = 0.0$, 1, 2, 3 and 7, **b** – $\Psi = \pi/4$, W_{22} – the same as in **a**

different values of astigmatism $W_{22} = n\lambda/\pi$, $n = 0.0$, 1.0, 2.0, 3.0 and 7.0 for $\Psi = \pi/8$ and $\pi/4$. The numerical results have been obtained for the mid-focal plane between the sagittal and tangential focii. It is observed that as the amount of aberration increases the peak irradiance decreases, the central fringe widens and curves start becoming flat.

Finally, we can conclude that the resolving power of the system, which is much less than that of an usual microscope of the same numerical aperture, is further reduced if the lenses are not well corrected. Secondly, one has to be very careful in the selection of quadrature scheme for evaluating the integrals of the type such as those in Eq. (7) which is highly oscillatory in nature. As pointed out by BARAKAT [31], the Gauss quadrature method is good for OTF calculations and gives a good accuracy with 20-points. But, in the imaging calculations, one must use more points. For oscillatory functions, modified Filon quadrature with slightly greater number of points is better than the Gauss quadrature. From economical point of view, Filon/FFT etc. quadrature scheme should be used. It will be of much use if the sampling theorem [34] is extended for the non-rotationally symmetric systems.

Acknowledgements — We wish to thank Prof. A. K. Ghatak for his interest in the work.

References

[1] KUBOTA H., INOUE S., J. Opt. Soc. Am. **49** (1959), 191.
[2] KUBOTA H., SAITO H., J. Opt. Soc. Am. **50** (1960), 1020.
[3] KATTI P. K., SINGH K., CHOPRA K. N., Appl. Opt. **9** (1970), 1379.
[4] KATTI P. K., SINGH K., CHOPRA K. N., Opt. Acta **17** (1970), 439.
[5] ASAKURA T., SUZUKI T., Jap. J. Appl. Phys. **4**, Suppl. 1, (1965), 267.
[6] DALBERRA J. P., Nouv. Rev. Opt. Appl. **2** (1971), 255.
[7] SINGH J., SINGH K., Opt. Acta **23** (1976), 161.
[8] SINGH K., SINGH J., Microscop. Acta **78** (1976), 149.
[9] GUPTA K. K., BAHUGUNA R. D., SINGH K., Microscop. Acta **80** (1977), 37.
[10] BARAKAT R., Opt. Acta **27** (1980), 847.
[11] BORN M., WOLF E., *Principles of Optics*, Pergamon Press, 1975.
[12] KAPANY N. S., BURKE J. J., J. Opt. Soc. Am. **52** (1962), 1351.
[13] BARAKAT R., HOUSTON A., J. Opt. Soc. Am. **55** (1965), 1132.
[14] YOSHIDA A., ASAKURA T., Opt. Commun. **25** (1978), 133.
[15] GUPTA A. K., SINGH R. N., SINGH K., Can. J. Phys. **55** (1977), 1025.
[16] GUPTA A. K., SINGH K., Microscop. Acta **80** (1978), 359.
[17] POWELL I., Opt. Acta **20** (1973), 879.
[18] SHEPPARD C., Jr., WILSON T., Appl. Opt. **18** (1979), 1058.
[19] HOFMANN C., PABST S., Exp. Tech. Phys. **26** (1978), 87.
[20] YZUEL M. J., BESCOS J., Opt. Acta **23** (1976), 529.
[21] BISWAS S. C., BOIVIN A., J. Optics (India) **4** (1975), 1.
[22] BISWAS S. C., BOIVIN A., Can. J. Phys. **57** (1979), 1388.
[23] HAZRA L. N., Can. J. Phys. **57** (1979), 1340.
[24] YZUEL M. J., CALVO F., Opt. Acta **26** (1979), 1379.
[25] MAGIERA A., MAGIERA L., PLUTA M., Optik **53** (1979), 343.
[26] MAGIERA A., MAGIERA L., PLUTA M., Optik **56** (1980), 413.

[27] TANGO W. J., Appl. Phys. **13** (1977), 327.
[28] BARAKAT R., J. Opt. Soc. Am. **70** (1980), 739.
[29] BUDGOR A. B., Appl. Opt. **19** (1980), 1597.
[30] HOPKINS H. H., YZUEL M. J., Opt. Acta **17** (1970), 157.
[31] BARAKAT R., [in] *The Computer in Optical Research*, Springer–Verlag 1980.
[32] YZUEL M. J., ARLEGUE F. J., Opt. Acta **27** (1980), 549.
[33] BARAKAT R., J. Opt. Soc. Am. **54** (1964), 920.
[34] FRIEDEN B. R., J. Opt. Soc. Am. **56** (1966), 1355.
[35] WATSON G., *A Treatise on Bessel Function*, Cambridge University Press, 1944.

Received November 6, 1986

Влияние аберрации третьего ряда на пунктирную функцию размыва в поляризационном микроскопе с пересекающимися поляризаторами

Исследовано влияние аберрации третьего ряда (spherical, coma and astigmatism) на распределение интенсивности в образе пунктирного предмета для поляризационного предмета с пересекающимися поляризаторами. Даны детальные результаты указывающие на ухудшение образа при аберрации по поводу уменьшения интенсивности в главном максимуме расширения образа. Проиллюстрирована степень улучшения при расфокусировке для системы со сферической аберрацией. В присутствии комы перемещение положения пика главного максимума повышается с её растущим значением.